

# ArcGIS™ Proximity and Cluster Analysis of Electron Probe Micro-Maps of Round Top Critical Mineral Deposit

Lorraine M. Negrón<sup>1</sup>, Margaret Piranian<sup>1</sup>, Maria A. Amaya<sup>2</sup>,  
Daniel Gorski<sup>3</sup>, Nicholas E. Pingitore<sup>1\*</sup>

<sup>1</sup>Department of Geological Sciences, The University of Texas at El Paso, El Paso, Texas, USA

<sup>2</sup>School of Nursing, The University of Texas at El Paso, El Paso, Texas, USA

<sup>3</sup>Texas Mineral Resources Corporation, Sierra Blanca, Texas, USA

Email: \*npingitore@utep.edu

**How to cite this paper:** Negrón, L.M., Piranian, M., Amaya, M.A., Gorski, D. and Pingitore, N.E. (2020) ArcGIS™ Proximity and Cluster Analysis of Electron Probe Micro-Maps of Round Top Critical Mineral Deposit. *Advances in Materials Physics and Chemistry*, 10, 63-76.

<https://doi.org/10.4236/ampc.2020.103006>

**Received:** December 30, 2019

**Accepted:** March 24, 2020

**Published:** March 27, 2020

Copyright © 2020 by author(s) and Scientific Research Publishing Inc. This work is licensed under the Creative Commons Attribution International License (CC BY 4.0).

<http://creativecommons.org/licenses/by/4.0/>



Open Access

## Abstract

Critical and rare earth elements are in high demand for their increasing incorporation in modern technological devices for applications in the military, industrial, commercial, and consumer sectors. Round Top Mountain, a rhyolite laccolith in Sierra Blanca, west Texas, U.S.A. is a unique mineral deposit that offers opportunity for development of rare earth elements, especially the heavy rare earths, as well as associated critical elements. The main objective here is to evaluate the distances between accessory minerals of potential economic value (yttriofluorite, cryolite, uraninite, thorite, cassiterite, and columbite), and to major (potassium feldspar, albite, and quartz) and minor minerals (annite mica, magnetite, and zircon). In this study we explore the proximity and clustering of these minor and accessory minerals, at the micron-to-millimeter scale, from mineral maps constructed in a previous application of ArcGIS™ tools to electron probe microanalysis (EPMA) element maps. Our goal is to determine whether specific minerals cluster spatially and, if so, at what distances. We noted that the high-value target yttriofluorite grains often neighbor potassium feldspar and quartz grains, but less commonly magnetite and mica grains. With regard to cluster analysis, most minor and accessory minerals were found to group together at small scales (low micrometer) and were dispersed or random at larger (up to 1 mm) distances.

## Keywords

ArcGIS™, EPMA, Proximity, Ripley's K-Function, Critical Minerals, Yttriofluorite, Round Top Deposit

## 1. Introduction

In this study, we examine minor and accessory minerals from a potentially economically valuable deposit of heavy rare earth elements (HREEs) and other critical elements [1]-[10]. Round Top Mountain is a rhyolite laccolith in Hudspeth County, west Texas, U.S.A. This Tertiary mushroom-shaped, peraluminous igneous intrusion has a mass estimated at 1.6 billion tons, and is approximately 2000 m in diameter and some 375 m in height. The major elemental composition of the rhyolite comprises Si, O, K, Al, and Na. This unique deposit underwent chemical alteration by a late-stage fluorine vapor phase that enriched it in HREEs and other incompatible elements [2] [6]. The laccolith exhibits exceptionally homogeneous mineralization [7], with rare earth element (REE) concentration over 500 ppm, of which the desirable yttrium + HREEs (YHREEs) comprise approximately 72%, making it of global significance [3] [11].

## Approach and Purpose

This research is an extension of previous work on the Round Top Mountain deposit in which multivariate statistical analysis (principal component analysis) converted electron microprobe elemental maps [8] into mineral maps [9]. In the current paper, those mineral maps are further analyzed spatially through proximity and cluster analyses using tools in the ArcGIS™ software system.

Multivariate spatial cluster analysis using ArcGIS™ has been applied in a variety of fields [12] [13] [14] [15]. Here proximity analysis evaluates the separation between yttrifluorite grains, and their proximity to other minor minerals. Cluster analysis demonstrates whether minor and accessory minerals exhibit clustering patterns and if so, at what distance or distance ranges. This approach employs Ripley's K function to show how spatial clustering or dispersion of feature centroids changes as neighborhood sizes increase.

The purpose of this study is to ascertain whether specific minerals of potential economic value are clustered or dispersed at the millimeter and lower distance scales in the rhyolite. The findings could improve our understanding of the mineralization process at Round Top Mountain and inform approaches to potential extraction of that mineral wealth.

## 2. Materials and Methods

### 2.1. Sample Collection and Preparation

Composite samples were obtained from reverse circulation drilling of Round Top Mountain rhyolite by Texas Mineral Resources Corporation, a publicly traded (stock ticker TMRC) junior mining explorer. TMRC was interested in testing this deposit and evaluating the mineralization of the rhyolite. Random rock fragments were chosen and thin sections were made by gluing each of those pieces to the surface of a glass petrographic slide, grinding them flat, and polishing and buffing them to a mirror finish [8].

## 2.2. Electron Probe Microanalysis

Using an electron probe micro-analyzer (EPMA), four thin sections were analyzed for 16 elements: Al, Ca, Dy, F, Fe, K, Na, Nb, Rb, Si, Sn, Th, U, Yb, Y, and Zr. The EPMA technique determines elemental compositions of individual grains or portions of grains in thin sections *via* a beam of accelerated electrons focused on a micrometer-sized site on the thin section. The beam of electrons interacts with the electrons of the elements and causes emission of characteristic X-rays of those elements [16]. The EPMA was a Cameca SX-50 (upgraded to SX-100 performance) with 4 wavelength dispersive spectrometers (WDS). Each randomly selected  $2 \times 2$  mm area on a thin section was WDS-raster-scanned repeatedly to yield a  $512 \times 512$  pixel elemental image or map. The quality of the resultant X-ray image depends on several factors, including the particular element, its concentration, dwell time of the beam on each pixel, and the beam current. Instrument settings were 20 KeV accelerating electron beam voltage and 200 or 250 nA current. Four mineral maps are seen in **Figure 1**, with yttrifluorite grains indicated.

## 2.3. ArcGis™ Proximity Analysis

The first analysis determined the distances between each of the yttrifluorite (YF)

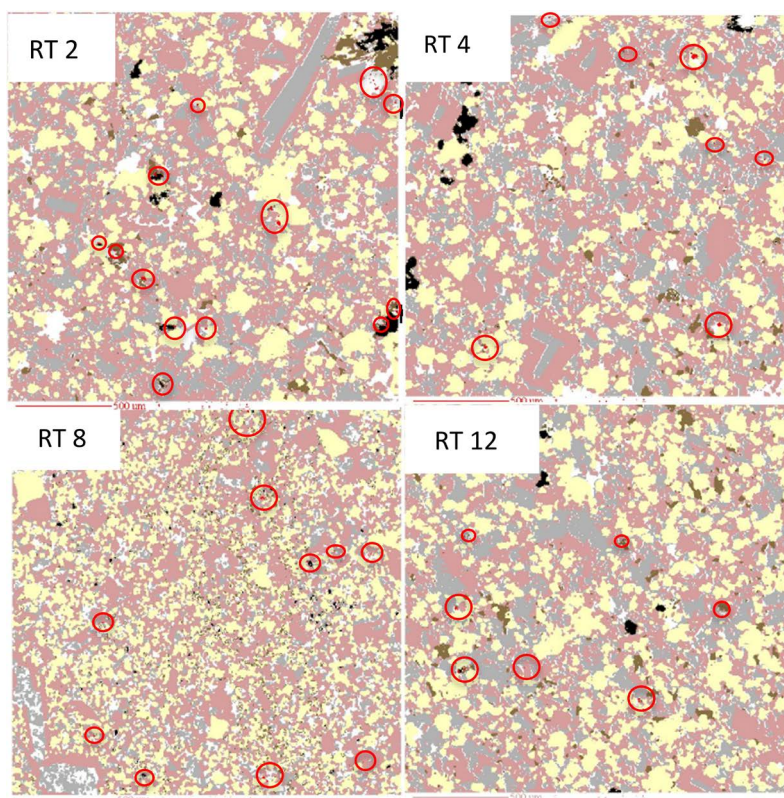


**Figure 1.** Mineral maps generated from electron probe microanalysis of 4 Round Top rhyolite samples. YF grains circled in red, some with multiple YF grains in close proximity. Mineral colors: K-spar (pink), albite (gray), quartz (yellow), magnetite (black) and anite mica (brown) and YF (red and circled). Field of View  $2 \text{ mm} \times 2 \text{ mm}$ .

grains in a map. One approach is to create buffers to surround each YF grain to assist in measuring the proximity between grains using feature classes. The buffer tool works by creating a buffer (ring) polygon at a user-specified distance. There are two types of buffers: Euclidean and geodesic. Due to the nature of our dataset and the custom reference frame that we had created, we used the Euclidean buffer, which measures in a two-dimensional Cartesian plane. The planar method suited our data and buffer distances of 1-, 10-, and 100- $\mu\text{m}$  were tested. The 1- and 10- $\mu\text{m}$  buffer distances proved appropriate to the small size of the yttrifluorite grains in the samples.

#### 2.4. ArcGis™ Cluster Analysis

The ArcGIS™ raster calculator tool created separate mineral maps by overlapping multiple individual element X-ray maps and correlating the pixels in which elements of a specific mineral occur together. These individual mineral maps then were converted from rasters to feature classes in order to use geo-processing spatial analysis tools. The feature classes were further studied by Multi-Distance Spatial Cluster Analysis (Ripley's K-function). This tool determines whether features exhibit statistically significant clustering or dispersion over a range of distances, and it requires "projected data" to accurately measure distances [17]. We created a custom projection of 2000  $\mu\text{m}$  by 2000  $\mu\text{m}$  using the Data Management toolbox and defining our own projection. To ensure statistical significance we used the 99.9% confidence interval (CI) for the smaller datasets and the 90% CI and 99% CI for larger datasets. The majority of the data reasonably fit within a distance of 300  $\mu\text{m}$  for all minerals and all samples using 99 permutations (99% CI) and 999 permutations (99.9% CI). A total of 60 distance bands was generated with a beginning distance of 5  $\mu\text{m}$ , increasing by increments of 5  $\mu\text{m}$  per iteration of the analysis.

We used Ripley's Edge Correction Formula for square and rectangular data because it checks each point's distance from the edge of the study area and its distance to each of its neighbors [17]. To be considered statistically significant, the observed K values must be above the higher confidence interval (clustering) or below the lower confidence interval (dispersion). K-values that fall between the confidence intervals and along the expected K-value line reflect a random distribution of the item of interest.

### 3. Results

#### 3.1. Proximity Analysis of Yttrifluorite

Yttrifluorite (YF) is a variety of fluorite ( $\text{CaF}_2$ , isometric) in which yttrium and REEs, particularly HREEs, substitute for up to some 30% of the Ca [18]. Because virtually all of the YHREEs at Round Top are hosted in YF [3], it is the target mineral for REE extraction. Map RT 8 has the largest number of yttrifluorite grains of the 4 maps studied (Table 1). The longest distance between yttrifluorite grains is 2000  $\mu\text{m}$  and the shortest distance is 17  $\mu\text{m}$ . The average distance

**Table 1.** Number, size, and neighbor proximity of Yttrifluorite grains.

Feature	Sample ID			
	RT 2	RT 4	RT 8	RT 12
# of YF grains	12	7	15	13
Smallest grain	2 $\mu\text{m}$	2 $\mu\text{m}$	4 $\mu\text{m}$	2 $\mu\text{m}$
Largest grain	24 $\mu\text{m}$	56 $\mu\text{m}$	40 $\mu\text{m}$	16 $\mu\text{m}$
Shortest distance	30 $\mu\text{m}$	30 $\mu\text{m}$	150 $\mu\text{m}$	20 $\mu\text{m}$
Longest distance	1600 $\mu\text{m}$	1925 $\mu\text{m}$	2000 $\mu\text{m}$	1150 $\mu\text{m}$
Average distance	737 $\mu\text{m}$	1008 $\mu\text{m}$	987 $\mu\text{m}$	723 $\mu\text{m}$
Mineral neighbors	K-spar, Qtz	K-spar, Qtz	K-spar, Qtz	K-spar, Magnetite

between YF grains for all four RT maps is 864  $\mu\text{m}$ . The important factor is the random dispersion of the yttrifluorite grains that possibly renders extraction of those grains by mechanical separation and concentration more difficult than if there were multiple grains in close proximity. At times the YF grains are spread randomly throughout the entire 2  $\times$  2 mm square map, creating the large variation in distances. In contrast, when the YF grains are found segregated to a certain quadrant of the thin section, the distance between grains shortens.

The minerals neighboring minerals the YF grains were also identified (**Table 1**). Knowledge of the neighboring minerals can inform the ease with which the yttrifluorite might be extracted by acid heap leaching, *i.e.*, whether the YF grains are proximal to soluble or to insoluble minerals. All samples showed some YF grains that are surrounded by minerals, feldspars and quartz, which are insoluble in the dilute sulfuric acid ( $\text{H}_2\text{SO}_4$ ) that has been proposed for YF extraction by heap leaching. There also are YF grains that are associated with Fe-bearing magnetite or hematite and annite mica grains; both these neighbors are soluble in dilute sulfuric acid. This is consistent with a previous study that showed an increase in pore space after exposure to sulfuric acid, which apparently assisted in the efficient leaching extraction of the YF-hosted REEs [5].

### 3.2. Ripley's K Cluster Analysis

In the figures that follow (**Figures 2-10**), the blue line represents the K-values expected for a random distribution of the specified mineral grains, the red line is the observed K-value for each distance, and the dotted lines are the upper and lower limits of the confidence envelope (99% or 99.9%). Points that fall above the expected blue line indicate clustering, but they are only significant if they are above the upper limit of the confidence envelope.

Ripley's K analysis is sensitive to the size of the project area under evaluation and our results reflect that in part. The choice of appropriate analysis parameters proved essential to prevent rendering graphs in which the axes reached 2000  $\mu\text{m}$ . At greater distances the confidence interval and observed k-values bent off the scale and thus were no longer valid.

### 3.2.1. Magnetite ( $\text{Fe}_3\text{O}_4$ , Isometric)

Magnetite is the fifth most common mineral found in Round Top rhyolite samples. Magnetite shows statistically significant clustering in RT 2 (in the distance range of 10 to 120  $\mu\text{m}$ ) and RT 4 (5 - 80  $\mu\text{m}$ ) samples (**Figure 2**). There is some clustering found in the RT 8 sample, also in the range of 10 - 80  $\mu\text{m}$ , whereas there is no clustering observed in RT 12. RT 2 and RT 4 show minimal statistically significant dispersion at large distances ranging from 232 - 300  $\mu\text{m}$  and 242 - 300  $\mu\text{m}$ , but neither RT 8 nor RT 12 shows any dispersion. With the exception of RT 2 and RT 4, it is notable that some clustering occurs at short distances but the mineral magnetite appears to be more randomly distributed.

### 3.2.2. Annite Mica ( $\text{K}(\text{Mg},\text{Fe})_3(\text{AlSi}_3\text{O}_{10})(\text{F},\text{OH})_2$ , Monoclinic)

Annite mica is the fourth most common mineral found throughout the Round Top rhyolite deposit and is important as the host of valuable lithium.

It displays significant short-distance clustering in the RT 2 and RT 4 samples (**Figure 3**). Grain clustering ranges from 5 - 150  $\mu\text{m}$  and 5 - 205  $\mu\text{m}$ , respectively. RT 8 exhibits statistically significant clustering that spans the entire scale from 5 - 300  $\mu\text{m}$ . Similarly, RT 12 also shows some clustering with distances from 5 - 110  $\mu\text{m}$  and again between 270 - 300  $\mu\text{m}$ . RT 2 shows dispersion at distances greater than 150  $\mu\text{m}$  and RT 4 at distances greater than 245  $\mu\text{m}$ . RT 8 and RT 12 do not show any dispersion.

### 3.2.3. Zircon ( $\text{ZrSiO}_4$ , Tetragonal)

Zircon, an accessory mineral, showed significant clustering for RT 2 between 18 - 50  $\mu\text{m}$ , RT 4 between 5 - 75  $\mu\text{m}$  and RT 12 between 8 - 60  $\mu\text{m}$  (**Figure 4**). RT 4 and RT 12 were closely related with significant clustering for a larger distance span than RT 2. RT 8 exhibited no clustering or dispersion from 25 - 300  $\mu\text{m}$ . RT

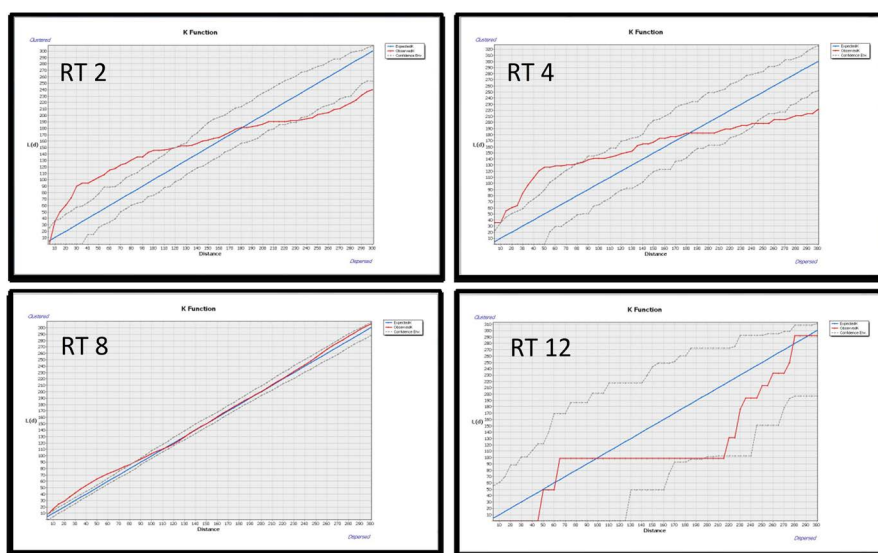


**Figure 2.** Cluster analysis results for magnetite. Distance (x-axis) vs. Ripley's K (y-axis). Expected K values (blue line), observed K values (red line), and confidence interval (dotted line).

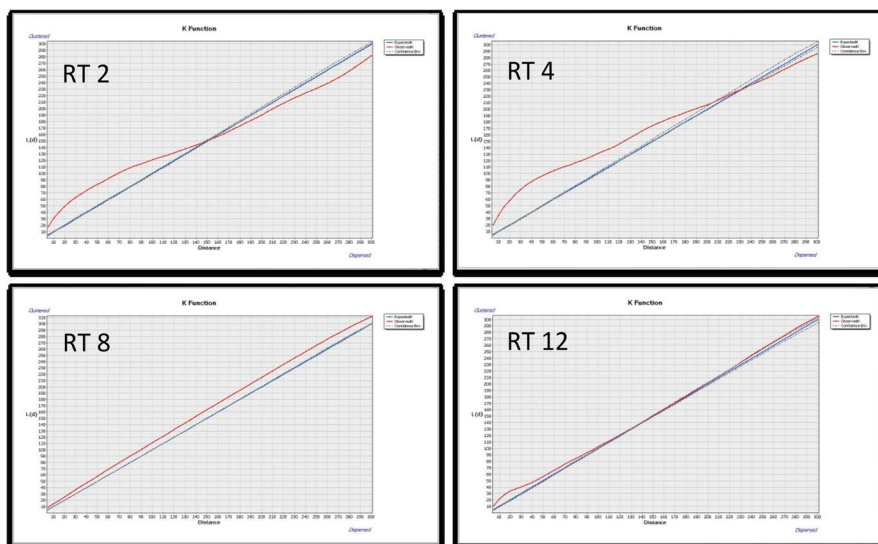


**Figure 3.** Cluster analysis for annite mica. Distance (x-axis) vs. Ripley's K (y-axis). Expected K values (blue line), observed K values (red line), and confidence interval (dotted line).

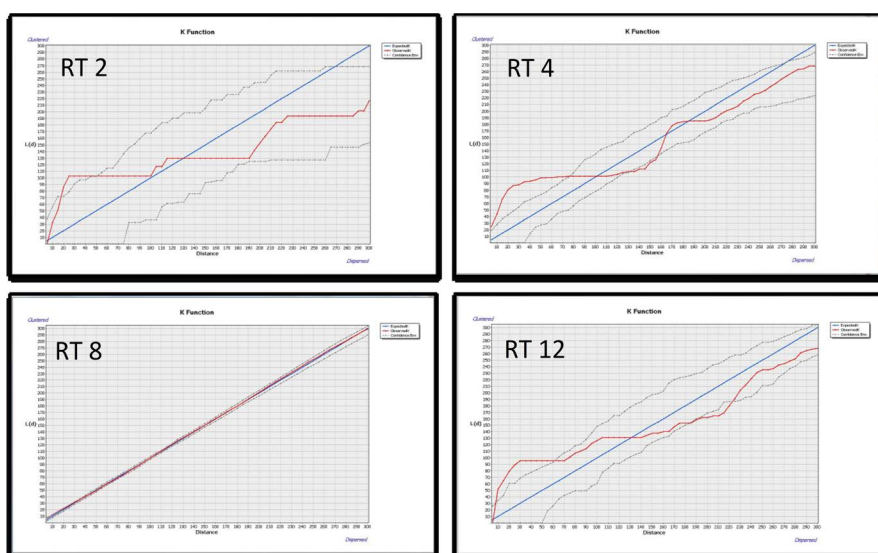


**Figure 4.** Cluster analysis for zircon. Distance (x-axis) vs. Ripley's K (y-axis). Expected K values (blue line), observed K values (red line), and confidence interval (dotted line).

4 and RT 12 displayed dispersion at some distance intervals; however, the majority of zircons are scattered in the four samples.

### 3.2.4. Yttriofluorite ((Ca,Y,HREE)F<sub>2</sub>, Isometric)

Although all four samples show statistical clustering, RT 2 stands out for its significant clustering over a large distance from 5 - 250  $\mu\text{m}$  (**Figure 5**). RT 4 has clustering between 5 and 55  $\mu\text{m}$ , while RT 8 also shows a staggered clustering pattern between 5 - 60  $\mu\text{m}$ . RT 12 exhibits clustering from 5-20  $\mu\text{m}$  but as noticed in **Figure 5**, RT 12 begins to bend off the expected k-value line (blue) that signifies that the results are statistically significant but analytically insignificant

for any points that falls in that boundary outlier. Data show that yttrifluorite tends to occur more in clusters than randomly or dispersed.

### 3.2.5. Cryolite ( $\text{Na}_3\text{AlF}_6$ , Monoclinic)

Cryolite has clustering for all four samples, beginning at short distances of  $5\ \mu\text{m}$  up to at least  $35\ \mu\text{m}$  (Figure 6). RT 2 ranged from  $5 - 70\ \mu\text{m}$ , RT 8 at  $5 - 110\ \mu\text{m}$  and RT12 had clustering up to  $130\ \mu\text{m}$ . RT 2 was the only sample that exhibited dispersion at two separate distance ranges:  $140 - 212\ \mu\text{m}$  and again at  $265 - 300\ \mu\text{m}$ . The other three samples showed no dispersion. Though cryolite shows some clustering and dispersion, the data more strongly suggest that cryolite occurs dispersed or randomly in samples RT 2 and 4. RT 8 and RT 12 observed k-values

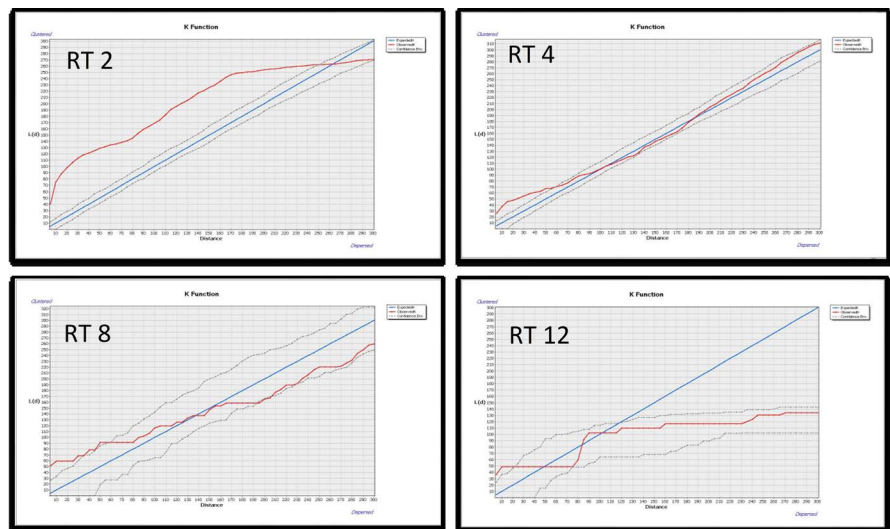


**Figure 5.** Cluster analysis for yttrifluorite. Distance (x-axis) vs. Ripley's K (y-axis). Expected K values (blue line), observed K values (red line), and confidence interval (dotted line).

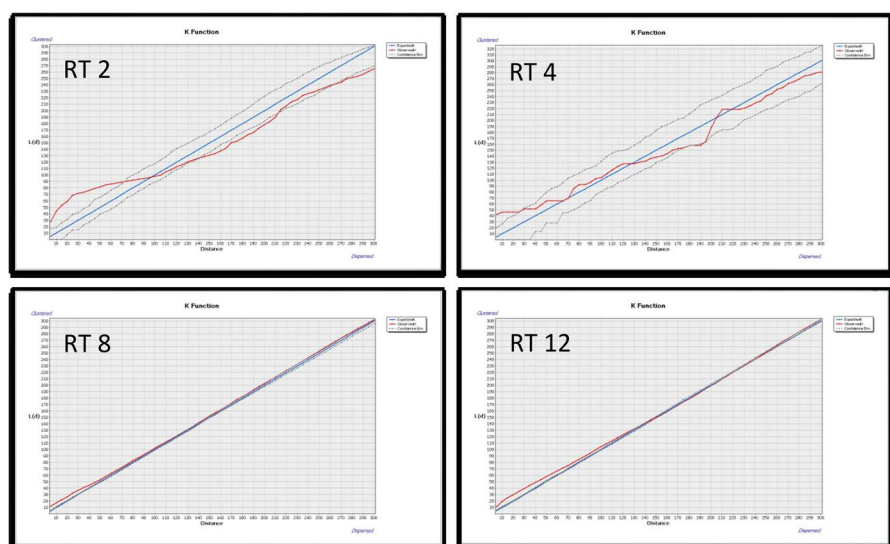


**Figure 6.** Cluster analysis for cryolite. Distance (x-axis) vs. Ripley's K (y-axis). Expected K values (blue line), observed K values (red line), and confidence interval (dotted line).

(red line) follow closely on the upper CI (dotted line) implying that for these samples, cryolite tends to develop in clusters.

### 3.2.6. Uraninite ( $\text{UO}_2$ , Isometric)

Although it is not abundant in these samples, uraninite grains show significant clustering in all four samples, at least up to distances between 5 - 25  $\mu\text{m}$ ; however, the levels of significance in the RT 8 and RT 12 samples are minimal compared to the other two (Figure 7). Only RT 2 and RT 12 show dispersion at larger distance and this occurs at two different intervals. RT 2 occurs dispersed between 170 - 198  $\mu\text{m}$  and again at 245 - 295  $\mu\text{m}$ , whereas RT 12 presented dispersion at 150 - 172  $\mu\text{m}$  and 212 - 285  $\mu\text{m}$ . Uraninite appears in clusters for shorter distances but is relatively dispersed or randomly distributed at longer distances in all samples.

### 3.2.7. Thorite ( $(\text{Th,U})\text{SiO}_4$ , Tetragonal)

RT 2 and RT 12 show similar statistically significant clustering at distances between 5 - 55  $\mu\text{m}$ . RT 8 does exhibit statistically significant clustering between 70 - 100  $\mu\text{m}$ ; but mostly it shows clustering that follows the upper CI level from 5 - 140  $\mu\text{m}$  where it crosses the expected k-values (blue line) and thorite becomes randomly distributed (Figure 8). RT 4 does not show any clustering but has random or dispersed distribution trends. Only RT 12 displays statistically significant dispersion from 260 - 285  $\mu\text{m}$ . Typically seen in close proximity to one another, thorite grains, like those of uraninite, also occur randomly distributed for all samples despite some statistically significant clustering found in RT 2 and RT 12.

### 3.2.8. Cassiterite ( $\text{SnO}_2$ , Tetragonal)

Statistically significant dispersion does not occur in any of the four samples; however, RT 4 and RT 12 have some statistically significant clustering (Figure 9).

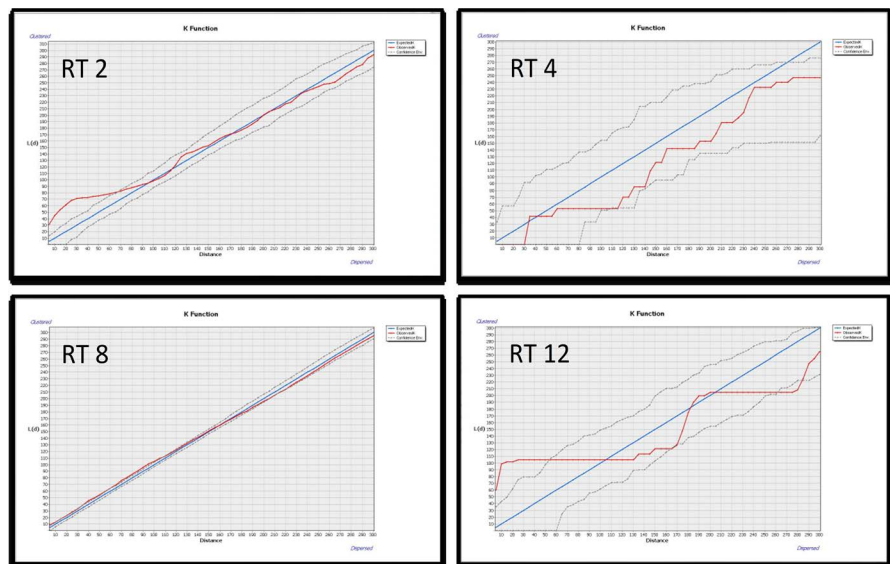


**Figure 7.** Cluster analysis for uraninite. Distance (x-axis) vs. Ripley's K (y-axis). Expected K values (blue line), observed K values (red line), and confidence interval (dotted line).

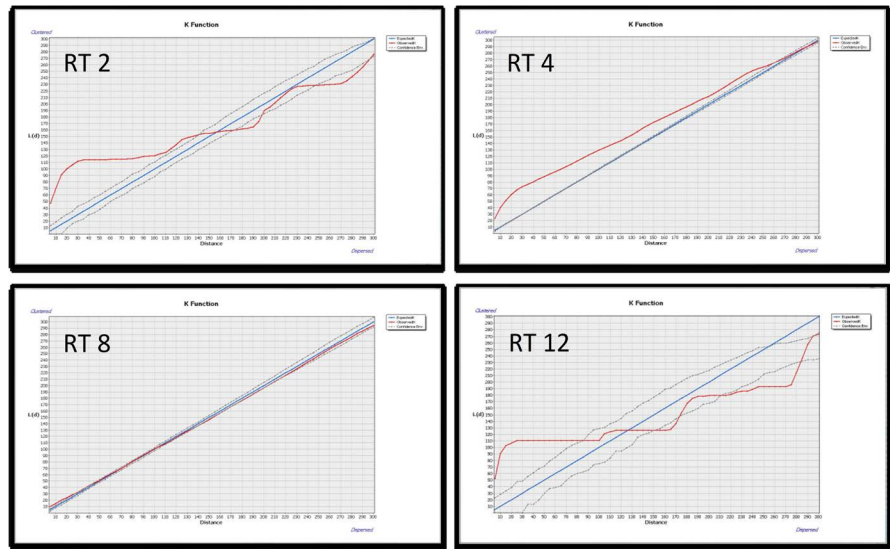


**Figure 8.** Cluster analysis for thorite. Distance (x-axis) vs. Ripley's K (y-axis). Expected K values (blue line), observed K values (red line), and confidence interval (dotted line).

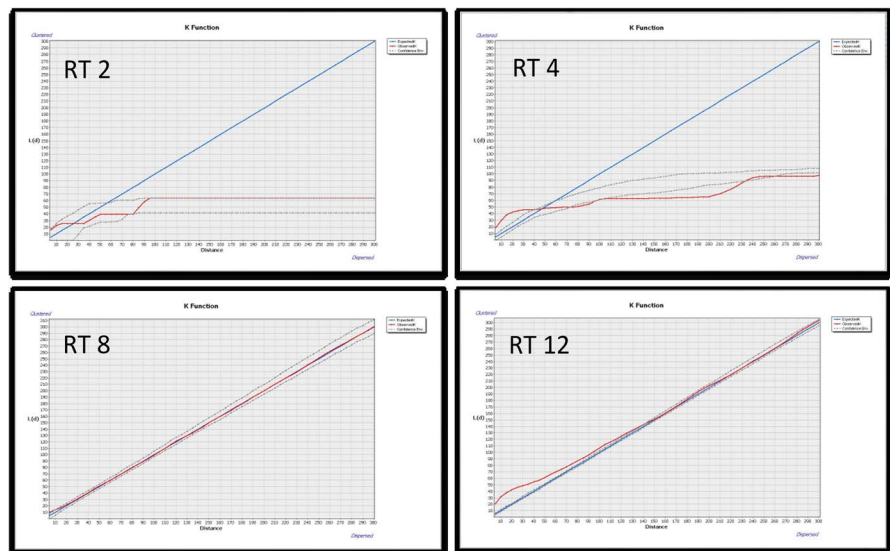


**Figure 9.** Cluster analysis for cassiterite. Distance (x-axis) vs. Ripley's K (y-axis). Expected K values (blue line), observed K values (red line), and confidence interval (dotted line).

RT 4 shows clustering between 5 - 40  $\mu\text{m}$  and RT 12 from 5 - 130  $\mu\text{m}$ . The data for cassiterite fall under 'statistical uncertainty' for RT 2 and RT 4 that have a bend in their data. RT 8 shows a random distribution for the majority of distance 20 - 300  $\mu\text{m}$  and RT 12 displays a similar trend at distances 150 - 180  $\mu\text{m}$  and 210 - 275  $\mu\text{m}$ .

### 3.2.9. Columbite ( $\text{Fe}^{2+}\text{Nb}_2\text{O}_6$ , Orthorhombic)

This mineral had 2 samples that show clustering at similar distances between 5 - 70  $\mu\text{m}$ , RT 2 and RT 12 (Figure 10). RT 2 has statistically significant clustering between 5 - 85  $\mu\text{m}$  and 115 - 165  $\mu\text{m}$ . Though not statistically significant, RT 2

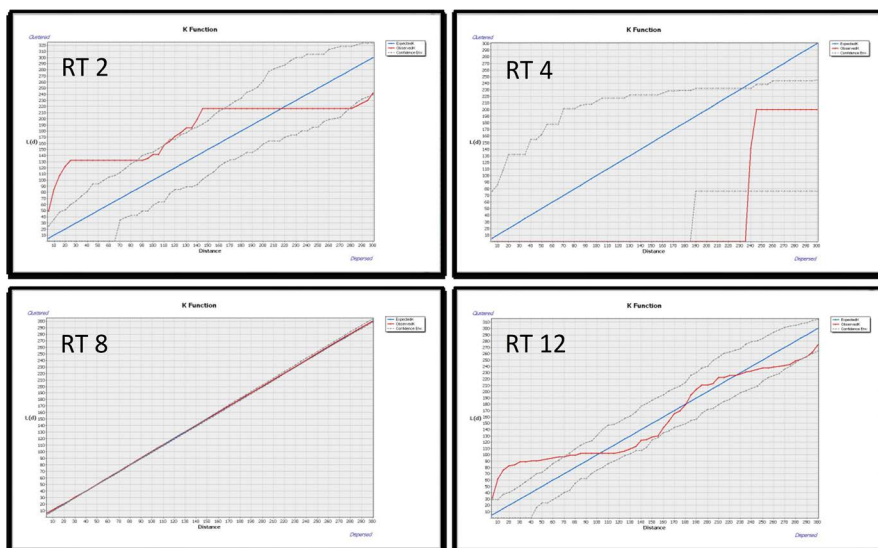


**Figure 10.** Cluster analysis for columbite. Distance (x-axis) vs. Ripley's K (y-axis). Expected K values (blue line), observed K values (red line), and confidence interval (dotted line).

does tend toward clustering from 5 - 200  $\mu\text{m}$  where it crosses to random and then dispersed distribution. Statistically significant dispersion occurred at large distances from 280 - 298  $\mu\text{m}$ . RT 4 did not display clustering at any distance but did have significant dispersion at distances between 185 - 238  $\mu\text{m}$  before values began to curve, rendering the remaining data invalid. The RT 8 sample curves are difficult to see; they appear to follow the expected K-values (blue line), a random distribution, from 15 - 300  $\mu\text{m}$ . Beyond that distance observed K-values follow the lower CI that relates to a dispersed distribution. Other than RT 2 that has statistically significant clustering for a large range in distance and RT 12 for a shorter range of distance, columbite exhibits either a random or dispersed spread in all samples at all distances.

#### 4. Conclusions

In an earlier work [9] we showed that overlaying the X-ray element maps in ArcGIS™ revealed element-mineral correlations to produce mineralogical maps. In this paper we described the use of those detailed maps to study the placement of minor and accessory minerals, relative to one another in order to understand mineral relationships at the micrometer-to-millimeter scale. Proximity and cluster analysis was performed on four mineral maps constructed using X-ray images produced by EPMA ArcGIS™ in order to determine point distances and construct clustering graphs.

Nine minor and accessory minerals were examined in these Round Top Mountain samples, of which yttrifluorite is of the most economic importance. Yttrifluorite occurs in clusters at short distances, between 5 - 20  $\mu\text{m}$ , or randomly spread throughout the  $2 \times 2$  mm areas of the rhyolite sampled. Proximity analysis of yttrifluorite, with respect to the four studied mineral maps, showed

that the shortest distance between individual YF grains or clusters is 30  $\mu\text{m}$  and the largest distance is 2000  $\mu\text{m}$ . Yttrifluorite grains neighbor potassium feldspar and quartz grains, and occasionally acid-soluble Fe-bearing minerals, chiefly magnetite and annite mica. YF grains in close proximity to one another suggest that the YF and other soluble minerals that lie near or conjointly, might be extractable simultaneously by acid heap leaching.

Further evaluation showed that clustering exists for all minerals; however, they do not necessarily cluster in all samples. Dispersion occurs for most minerals at greater distances, between 130 - 300  $\mu\text{m}$  but, again, not for every sample. Where clustering or dispersion was absent, minerals were distributed randomly throughout the sampled area. Sites where YF and other minor or trace minerals are in close proximity suggest that they were formed at the same time in this deposit. This information helps our understanding of how REE bearing minerals relate to one another and how potentially to extract those specific target minerals together. This clustering, especially near Fe-bearing minerals which are soluble with dilute sulfuric acid, could yield higher extraction of HREEs due to their close proximity and their proximity to pore space that will open as a result of the acid corrosion accompanying heap leaching of the deposit.

### **Acknowledgements**

The authors thank Texas Mineral Resources Corporation for providing access to proprietary technical data and samples. This project was supported by joint research contracts 26-8211-12 and 26-8211-16 between TMRC and the University of Texas at El Paso. Funds to cover the costs to publish in open access were obtained from this source. Also, we thank Dr. Ortolano and Ph.D. candidate Roberto Visalli from the University of Catania for access to their X-ray Map Analyzer application.

### **Disclosure**

L.M.N. and M.A.A. declared no potential conflicts and received no compensation for project participation. M.P., who managed the UTEP Microprobe Laboratory and performed the analyses, declares no potential conflicts. She received no extra compensation for participating in the project. D.G. is the CEO of TMRC and serves on its Board of Directors. N.E.P. serves on the Board of Directors of TMRC. He is not and has never been an employee of TMRC, nor has he received any compensation from the research contracts that supported this research. The funding sponsor, TMRC, had no role in the decision to publish the results.

### **Conflicts of Interest**

The authors declare no conflicts of interest regarding the publication of this paper.

### **References**

- [1] Rubin, J.N., Price, J.G., Henry, C.D. and Koppelaar, D.W. (1987) Cryolite-Bearing

- and Rare Metal-Enriched Rhyolite, Sierra Blanca Peaks, Hudspeth County, Texas. *American Mineralogist*, **72**, 1122-1130.
- [2] Price, J.G, Rubin, J.N., Henry, C.D., Pinkston, T.L., Tweedy, S.W. and Koppelaar, D.W. (1990) Rare-Metal Enriched Peraluminous Rhyolites in a Continental Arc, Sierra Blanca Area, Trans-Pecos Texas; Chemical Modification by Vapor-Phase Crystallization. GSA Special Papers No. 246, 103-120.  
<https://doi.org/10.1130/SPE246-p103>
- [3] Pingitore Jr., N.E., Clague, J.W. and Gorski, D. (2014) Round Top Mountain (Texas, USA) a Massive, Unique Y-Bearing-Fluorite-Hosted Heavy Rare Earth Element (HREE) Deposit. *Journal of Rare Earths*, **32**, 90-96.  
[https://doi.org/10.1016/S1002-0721\(14\)60037-5](https://doi.org/10.1016/S1002-0721(14)60037-5)
- [4] O'Neill, L.C. (2014) REE-Be-U-F Mineralization of the Round Top Laccolith, Sierra Blanca Peaks, Trans-Pecos Texas. University of Texas at Austin, Austin, TX.
- [5] Negrón, L., Pingitore Jr., N.E. and Gorski, D. (2016) Porosity and Permeability of Round Top Rhyolite (Texas, USA) Favor Coarse Crush Size for Rare Earth Element Heap Leach. *Minerals*, **6**, 16. <https://doi.org/10.3390/min6010016>
- [6] Elliott, B.A., O'Neill, L.C. and Kyle, J.R. (2017) Mineralogy and Crystallization History of a Highly Differentiated REE-Enriched Hypabyssal Rhyolite: Round Top Laccolith, Trans-Pecos, Texas. *Mineralogy and Petrology*, **111**, 569-592.  
<https://doi.org/10.1007/s00710-017-0511-5>
- [7] Pingitore Jr., N.E., Clague, J.W. and Gorski, D. (2018) Remarkably Consistent Rare Earth Element Grades at Round Top Yttrifluorite Deposit. *Advances in Materials Physics and Chemistry, Special Issue: Rare Earth Elements*, **8**, 1-14.  
<https://doi.org/10.4236/ampc.2018.81001>
- [8] Pingitore Jr., N.E., Piranian, M., Negrón, L. and Gorski, D. (2018) Microprobe Mapping of Rare Earth Element Distribution in Round Top Yttrifluorite Deposit. *Advances in Materials Physics and Chemistry, Special Issue: Rare Earth Elements*, **8**, 15-31. <https://doi.org/10.4236/ampc.2018.81002>
- [9] Negrón, L.M., Piranian, M., Amaya, M.A., Gorski, D. and Pingitore, N.E. (2020) ArcGIS™ and Principal Component Analysis of Probe Data to Micro-Map Minerals in Round Top Rare Earth Deposit. *Advances in Materials Physics and Chemistry*, **10**, 39-52. <https://doi.org/10.4236/ampc.2020.102004>
- [10] Gustavson Associates (2019) NI 43-101 Preliminary Economic Assessment: Round Top Project, Sierra Blanca, Texas.  
<http://tmrcorp.com/resources/reports/TMRC-NI43-101-PEA-2019-16-August-2019.pdf>
- [11] Jowitt, S.M., Medlin, C.C. and Cas, R.A.F. (2017) The Rare Earth Element (REE) Mineralisation Potential of Highly Fractionated Rhyolites: A Potential Low-Grade, Bulk Tonnage Source of Critical Metals. *Ore Geology Reviews*, **86**, 548-562.  
<https://doi.org/10.1016/j.oregeorev.2017.02.027>
- [12] Lee, Y. and Song, Y. (2007) Selecting the Key Research Areas in Nano-Technology Filed Using Technology and Cluster Analysis: A Case Study Based on National R&D Programs in South Korea. *Technovation*, **27**, 57-64.  
<https://doi.org/10.1016/j.technovation.2006.04.003>
- [13] Zhang, L., Lui, X., Janssens, F., Liang, L. and Glänzel, W. (2010) Subject Clustering Analysis Based on ISI Category Classification. *Journal of Informetrics*, **4**, 185-193.  
<https://doi.org/10.1016/j.joi.2009.11.005>
- [14] Anju, M. and Banerjee, D.K. (2012) Multivariate Statistical Analysis of Heavy Met-

- als in Soils of Pb-Zn Mining Area, India. *Environmental Monitoring and Assessment*, **184**, 4191-4206. <https://doi.org/10.1007/s10661-011-2255-8>
- [15] Ma, L., Sun, J., Yang, Z. and Wang, L. (2015) Heavy Metal Contamination of Agricultural Soils Affected by Mining Activities Around the Ganxi River in Chenzhou, Southern China. *Environmental Monitoring and Assessment*, **187**, 731. <https://doi.org/10.1007/s10661-015-4966-8>
- [16] Khashgerel, B., Kavalieris, I. and Hayashi, K. (2008) Mineralogy, Textures, and Whole-Rock Geochemistry of Advanced Argillic Alteration: Hugo Dummett Porphyry Cu-Au Deposit, Oyu Tolgoi Mineral District, Mongolia. *Mineralium Deposita*, **43**, 913-932. <https://doi.org/10.1007/s00126-008-0205-3>
- [17] Mitchell, A. (2005) *The ESRI Guide to GIS Analysis*, 2. ESRI Press, New York.
- [18] Mindat (2019) Yttrifluorite. <https://www.mindat.org/min-4371.html>